

Article

Impact of a Porous Si-Ca-P Monophasic Ceramic on Variation of Osteogenesis-Related Gene Expression of Adult Human Mesenchymal Stem Cells

Rabadan-Ros Ruben ^{1,*} , Revilla-Nuin Beatriz ², Mazón Patricia ³ , Aznar-Cervantes Salvador ⁴ , Ros-Tarraga Patricia ¹, De Aza Piedad N. ⁵  and Meseguer-Olmo Luis ¹ 

¹ Tissue Regeneration and Repair Group: Orthobiology, Biomaterials and Tissue Engineering, UCAM-San Antonio Catholic University of Murcia, Guadalupe, 30107 Murcia, Spain; p.ros.tarraga@gmail.com (R.-T.P.); lmeseguer.doc@gmail.com (M.-O.L.)

² Genomic Unit, Biomedical Research Institute of Murcia (IMIB-Arrixaca-UMU), University Clinical Hospital "Virgen de la Arrixaca", University of Murcia, El Palmar, 30120 Murcia, Spain; brevilla_nuin@yahoo.es

³ Department of Materials, Optics and Electronic Technology, Miguel Hernández University, Avda. Universidad s/n, Elche, 03202 Alicante, Spain; pmazon@umh.es

⁴ Department of Biotechnology, Instituto Murciano de Investigación y Desarrollo Agrario y Alimentario (IMIDA), La Alberca, 30150 Murcia, Spain; sdac1@um.es

⁵ Institute of Bioengineering, Miguel Hernández University, Avda. Universidad s/n, Elche, 03202 Alicante, Spain; piedad@umh.es

* Corresponding author: rubenrabadanros@gmail.com; Tel.: +34-620-754-831

Received: 4 December 2017; Accepted: 21 December 2017; Published: 1 January 2018

Abstract: This work evaluates *in vitro* the influence of a new biocompatible porous Si-Ca-P monophasic ($7\text{CaO}\cdot\text{P}_2\text{O}_5\cdot2\text{SiO}_2$) ceramic on the cellular metabolic activity, morphology and osteogenic differentiation of adult human mesenchymal stem cells (*ahMSCs*) cultured in basal growth medium and under osteogenic inductive medium. Alamar Blue Assay and FESEM were carried out in order to monitor the cell proliferation and the shape of the cells growing on the Si-Ca-P monophasic ceramic during the study period. The osteogenic differentiation of *ahMSCs* was investigated by means of immunofluorescent staining (osteocalcin, osteopontin, heparan sulphate and collagen type I expression), quantitative reverse transcription polymerase chain reaction (qRT-PCR) (integrin-binding sialoprotein, osteocalcin, alkaline phosphatase, osteopontin, osteonectin, runt-related transcription factor 2 and collagen type I) and expression of surface markers (CD73, CD90 and CD105). We could check osteogenic differentiation in *ahMSCs* growing under the influence of Si-Ca-P monophasic ceramics itself, but especially when growth medium was replaced by osteogenic medium in the culture conditions. These results allowed us to conclude that the new Si-Ca-P monophasic scaffold greatly enhanced *ahMSCs* proliferation and osteogenic differentiation; therefore, it may be considered to be employed as a new bone graft substitute or scaffold for bone tissue engineering.

Keywords: bioceramics; Si-Ca-P based materials; mesenchymal stem cells; osteogenic differentiation; tissue engineering

1. Introduction

Tissue engineering can be conceptualized as the use of a combination of cells, materials, and biochemical and physicochemical factors to improve or replace biological tissues [1]. Based on this, bone tissue repair-regeneration has been the focus and may be one the major applications of this discipline. A great number of strategies have been evolved over the past decades towards engineering tissue replacements, but the most common approach implies the use of reabsorbable synthetic materials

as scaffolds acting as a 3D-framework for cell growth in vitro. An ideal synthetic matrix for bone regeneration should fulfill some requirements as being bioactive and reabsorbed at medium term, displaying mechanical characteristics similar to bone tissue and, at the same time, possessing the ability to enhance cell proliferation while supporting tissue specific differentiation [2].

Among various biomaterials, calcium phosphate-based ceramics (CaP) play a critical role as scaffold in bone tissue engineering. Previously, from 1960 to 1970, these materials have been widely used to repair bone defects because of their properties of biocompatibility, safety, unlimited availability, high cost-effectiveness ratio and similarity to mineral fraction of the bone [3]. CaP ceramics can be used alone or in combination with other ceramics or compounds as proteins or polymers [4,5]. The biphasic CaP ceramics have some advantages over simple-phase ceramics by presenting favourable bioactivity and controllable biodegradation in vivo [6]. Besides, they can be used as a vector for therapeutic molecules. Alternatively, it has been demonstrated that they integrate directly in host bone tissue through formation of an apatite interface layer [7]. CaP ceramics can promote osteogenic cellular activities, mineral deposition and bone formation. Furthermore, the mineralization of the surface of these ceramics to form the apatite layer may facilitate quick protein fixing on the surface and consequently, promote cell adhesion, proliferation and osteogenic differentiation. For this reason, the surface mineralization prior to implantation by means of the use of simulated body fluid (SBF) may increase the bioactivity to improve the osteointegration with the host bone [8].

The incorporation of specific ions into the chemical composition of bioceramics is expected to improve bone stimulating features. Silicon (Si) in CaP-based materials may play an important role in cell growth on the materials [9,10]. Si is recognised because of its unique effect on osteoblastic differentiation and thus bone mineralization [11].

Consequently, we have focused our attention on synthesizing a novel porous Si-Ca-P monophasic ceramic (SCP-c) by means of a solid-state reaction that was able to induce calcium deficient hydroxyapatite mineralization in simulated body fluid through the formation of two well differentiated Si-Carbonate-Hydroxyapatite layers [12]. Moreover, its properties of degradability and stimulation of bone tissue formation [13] indicated that the ceramic material possesses osteoconductive in vivo properties. The traditional in vitro techniques evidenced the biocompatibility of the SCP-c and its potential ability to stimulate osteogenic differentiation [14]. However, little has been studied in depth about the impact on the osteogenic differentiation of a primary adult human mesenchymal stem cells (*ahMSCs*) culture. In order to ensure that this new biomaterial induces *ahMSCs* differentiation to osteoblasts and to know the route by which it acts, in this work we have investigated and monitored the expression of genetic markers involved in the osteogenic differentiation of *ahMSCs* as well as the expression of different proteins of the extracellular matrix and surface markers (surface antigens) to give greater consistency to our results.

2. Materials and Methods

2.1. Preparation of Porous Si-Ca-P Monophasic Ceramic (SCP-c)

SCP-c powder was synthetized in our laboratory, according to a previously described processing method [3]. For specific information related to its mechanical behavior and physicochemical characterization, please consult the following publications [15,16]. The ceramic was synthetized from commercial-grade calcium hydrogen phosphate anhydrous (CaHPO₄; Panreac S.L.U., Barcelona, Spain), calcium carbonate (CaCO₃ > 99.0 wt %; Fluka-Sigma Aldrich Quimica SL, Madrid, Spain) with an average particle size of 13.8 µm, and silicon oxide (SiO₂ > 99.7 wt %; Strem Chemicals UK Ltd., Cambridge, UK) with an average particle size <50 µm. We can briefly describe the process of obtaining the porous Si-Ca-P material as a solid state reaction from the above-mentioned stoichiometric products that were homogenized, milled and isostatically preset, followed by a thermal treatment at 1300 °C/3 h and annealing at 1200 °C/24 h.

For the present investigation, SCP-c was cut in disc shapes of 7 mm in diameter and 3 mm in length, and gas-plasma was used for sterilization (Sterrad-1005TM, ASP, Irvine, CA, USA). Immediately before its use, each disk was placed in a well of a 24-well plate containing fetal bovine serum (FBS) (Sigma, St. Louis, MO, USA) and incubated at 37 °C for 1 h in a cell culture incubator to favour cell adhesion to the surface of the material. After that, disks were dried under dry heat at the same temperature.

2.2. Isolation, Characterization and Primary Culture of Adult Human Bone Marrow-Derived Mesenchymal Stem Cells (*ah*MSCs)

*ah*MSCs were isolated as previously described [17] and characterized following the criteria of International Society of Cell Therapy (ISCT) [18] (data not shown).

After cell expansion, *ah*MSCs of passage 3 (P3) were prepared for use in all subsequent experiments. For examination of attachment and proliferation assays, cells were seeded onto the top of disc-shaped SCP-c at a density of 5×10^3 cells·cm⁻² in a 48-well plate and cultured with growth medium (GM) which consists of Dulbecco's Minimal Essential Medium (DMEM) (Sigma-Aldrich, St. Louis, MO, USA) supplemented with 10% (*v/v*) FBS and routine antibiotics (penicillin/ streptomycin). To conduct osteogenic differentiation studies, three SCP-c scaffolds were placed in transwell inserts in 6-well plates (Sigma-Aldrich, Corning, NY, USA) and *ah*MSCs were seeded on the bottom of the wells at a density of 5×10^3 cells cm⁻² and cultured with GM. Cells seeded onto tissue culture-treated polystyrene (TCPS) culture plate (Sigma-Aldrich, Corning, NY, USA) served as a positive control.

Plates were incubated at 37 °C in a humidified atmosphere consisting of 95% air and 7.5% CO₂. Some of the *ah*MSCs cell cultures were also induced to osteogenic differentiation replacing the GM by osteogenic differentiation medium (OM) from the 21st day, which consisted of the GM supplemented with l-ascorbic acid-2-phosphate (0.2 mM; Sigma-Aldrich, St Louis, MO, USA), dexamethasone (10 nM; Sigma-Aldrich, Corning, NY, USA), and β-glycerolphosphatethe (10 nM; Merck, Darmstadt, Germany).

2.3. Field Emission Scanning Electron Microscopy (FESEM)

After 7, 14, 21 and 28 days of seeding, FESEM was used to examine cell attachment and proliferation. After fixing with glutaraldehyde (Sigma-Aldrich, Corning, NY, USA), scaffolds were dehydrated with ethanol, critical point dried with liquid CO₂ and then examined by FESEM Microscopy (Merlin™ VP Compact, Carl Zeiss Microscopy S. L., Oberkochen, Germany) after coating with gold.

2.4. Cellular Metabolic Activity Assay

Alamar Blue (Invitrogen, Carlsbad, CA, USA) was used to assess the metabolic activity of the *ah*MSCs at 7, 14, 21 and 28 days after the seeding. Fresh medium (200 µL) containing 10% (*v/v*) of Alamar Blue reagent was added to each well for 4 h at 37 °C in darkness. The fluorescence was read directly in a Synergy MX ultraviolet visible (UV-Vis) spectrophotometer (Bio Tek Instruments Inc., Winooski, VT, USA) at excitation and emission wavelengths of 560 and 590 nm, respectively.

2.5. Osteogenic Differentiation Assays

The ability of *ah*MSCs to differentiate into osteoblastic lineage cells was studied at 7, 14, 21 and 28 days by immunofluorescence staining (heparin sulphate, osteocalcin and collagen type I), expression of representative *ah*MSCs surface markers (CD73, CD90 and CD105) and quantitative real-time polymerase chain reaction (qRT-PCR) assay for osteogenic markers.

2.5.1. Immunofluorescence Staining Assay: Heparan Sulphate (HS), Osteocalcin (OCN), Osteopontin (OPN) and Collagen Type I (Col I) Expression

For immunofluorescence staining of HS, OCN, OPN and Col I, cells were fixed with 4% formaldehyde at 4 °C, and permeabilized with cooled Methanol–Acetone solution (1:1) (Sigma-Aldrich,

St. Louis, MO, USA) at 20 °C for 10 min. Labelling and visualization were performed as previously described [14].

2.5.2. Surface Markers Cluster Differentiation (CD)

The cells were detached from the culture flasks and centrifuged. Then, they were resuspended in buffer (2% FBS, 0.1% NaN₃ in PBS 1X (Sigma-Aldrich, Corning, NY, USA)) and counted. Aliquots of 1×10^5 cells were made in 25 µL of buffer into 3 tubes. Antibodies (CD90-FITC, CD73-PE and CD105-Alexa Fluor 647 and isotypes as negative controls) (Becton Dickinson Co., Franklin Lakes, NJ, USA.) were added at the dilution standardised by our laboratory and incubated at 4 °C for 30 min darkness. Cells were washed, and kept at 4 °C, before analysis by FACSCanto (Becton-Dickinson, Franklin Lakes, NJ, USA).

2.5.3. Osteogenic Gene Expression: Quantitative Real-Time Polymerase Chain Reaction (qRT-PCR) Assay

qRT-PCR assay was performed to analyse the expression of integrin-binding sialoprotein (IBSP), osteocalcin (BGLAP), alkaline phosphatase(ALPL), osteopontin (SPP1), osteonectin (SPARC), runt-related transcription factor 2 (RUNX2) and collagen type I (COL1A1). Total RNA was extracted from cells using a RNAqueous Micro Kit (Invitrogen by Thermo Fisher Scientific, Waltham, MA, USA) according to the manufacturer's instruction, followed by reverse transcription of mRNA with the iScript cDNA Synthesis kit (Bio-Rad). Quantitative PCR was carried out by using the mix SYBR Premix ExTaq (Takara) in an iCycler MyiQ thermocycler (Bio-Rad). Specific primers for mRNA were purchased from Qiagen (QuantiTech Primer Assays, Hilden, Germany).

For each primer set, the efficiency was >95%, and a single product was observed using melt curve analysis. Samples were run in duplicate, and the presented relative gene expression levels were calculated using the $2^{-\Delta C_t}$ method by normalizing to glyceraldehyde-3-phosphate dehydrogenase (GAPDH) (Qiagen, Hilden, Germany).

3. Calculation

All assays were performed at least in triplicate. Student's t-test was used to determine significant differences between groups (*p*-value < 0.05). All data are reported as mean ± standard deviation (SD).

4. Results

4.1. Field Emission Scanning Electron Microscopy (FESEM)

In order to evaluate adhesion and morphology of *ah*MSCs growing on SCP-c, the scaffolds cultured were examined by FESEM at days 7, 14, 21 and 28 after the seeding in GM and just at 28 days in OM.

By day 7 after the seeding (Figure 1A), the cells showed an initial spreading and the majority of the cells were stretched, but still exhibited some spherical forms.

After 14 days (Figure 1B), *ah*MSCs seeded on the material covered much of the surface and showed a fibroblastic appearance. At 28 days (Figure 1D,E), the cells occupied the entire surface, forming a monolayer. There are not cytotoxicity signals or morphological alterations throughout the study. Morphological differences were observed between cells cultivated with GM (Figure 1D) and OM (Figure 1E). The appearance of the cells treated with OM showed polygonal shapes like osteoblastic cells.

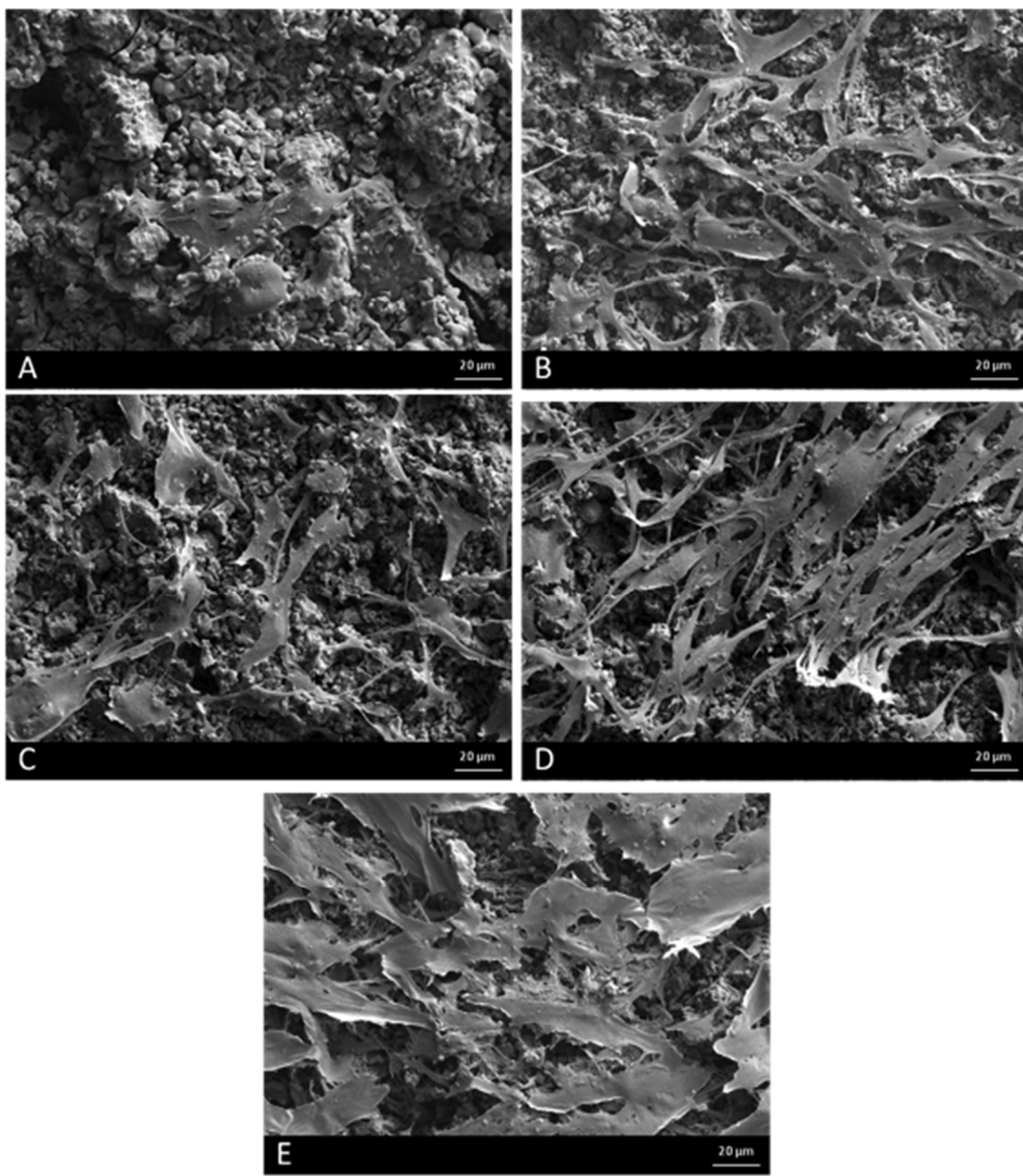


Figure 1. Representative FESEM images of the *ah*MSCs cells grown on ceramic surfaces at 7 days (A), 14 days (B), 21 days (C), 28 days (D) in GM and at 28 days in OM (E) (Original magnification: bar 20 μ m).

4.2. Cellular Metabolic Activity Assay

Figure 2 shows results of cellular metabolic activity as fluorescence arbitrary units (a.u.). The cells seeded on plastic (control) showed higher metabolic activity than *ah*MSCs cultured on SCP-c. Cell proliferation in the presence of SCP-c was inhibited for the first 2 weeks.

On day 21, significantly higher metabolic activity (*t*-test, $p < 0.05$) was observed compared with previous measurements. Remarkably, *ah*MSCs cultured on SCP-c with OM showed major metabolic activity than cells cultured with GM (*t*-test, $p < 0.05$).

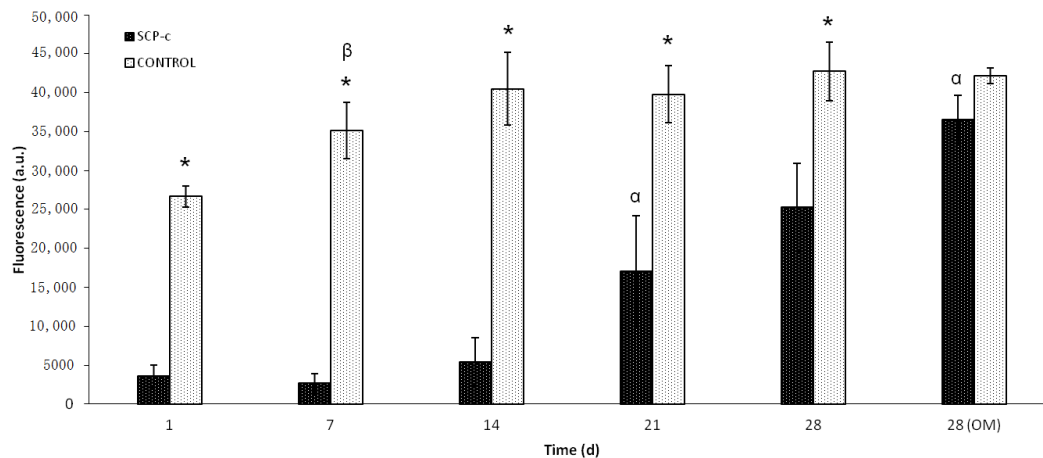


Figure 2. Cellular metabolic activity of the cells seeded on the SCP-c scaffolds compared to cell cultures on plastic (positive controls) obtained by means of Alamar Blue Assay. (*) denotes significant differences ($p < 0.05$) between SCP-c and the control for the same experimental time; (α) denotes significant differences ($p < 0.05$) between different experimental times obtained for cells growing on SCP-c scaffolds; (β) denotes significant differences ($p < 0.05$) between different experimental times obtained for control samples.

4.3. Differentiation Assays

4.3.1. Immunofluorescence Staining Assay: Heparan Sulphate (HS), Osteocalcin (OCN), Osteopontin (OPN) and Collagen Type I (Col I) Expression

Figure 3 shows immunofluorescence staining of HS, OCN, OPN and Col I from the extracellular matrix produced by *ah*MSCs at the end of the experiment (28 days) and 28 days under a week of influence of OM. After 28 days of culture, the cells cultured as control (left column of each chart) without any stimulus emit lower fluorescence in the Col I and HS staining than the cells seeded in indirect contact with SCP-c scaffolds. Moreover, the cells seeded in indirect contact with SCP-c scaffolds (right column of each chart) showed increasing fluorescence intensity in the HS, OCN, OPN and Col I staining with the addition of OM, being especially intense in the labeling of OPN. In addition, the cells acquired a rounded shape after incorporating OM.

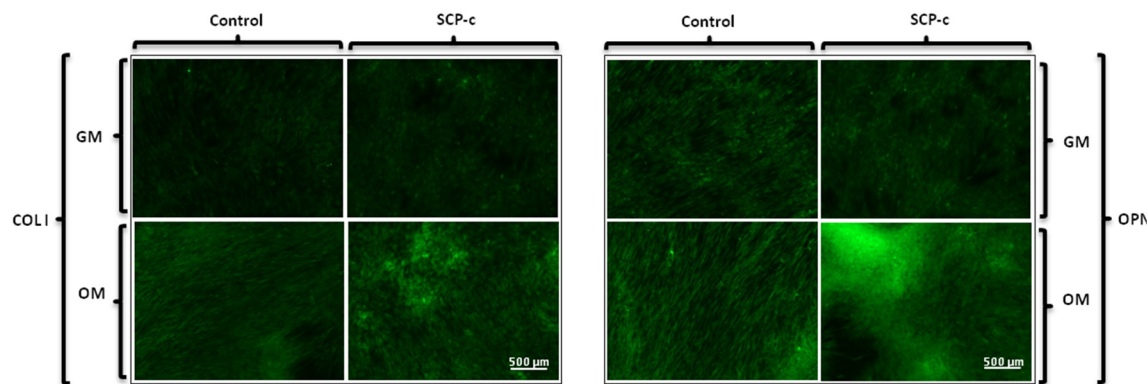


Figure 3. Cont.

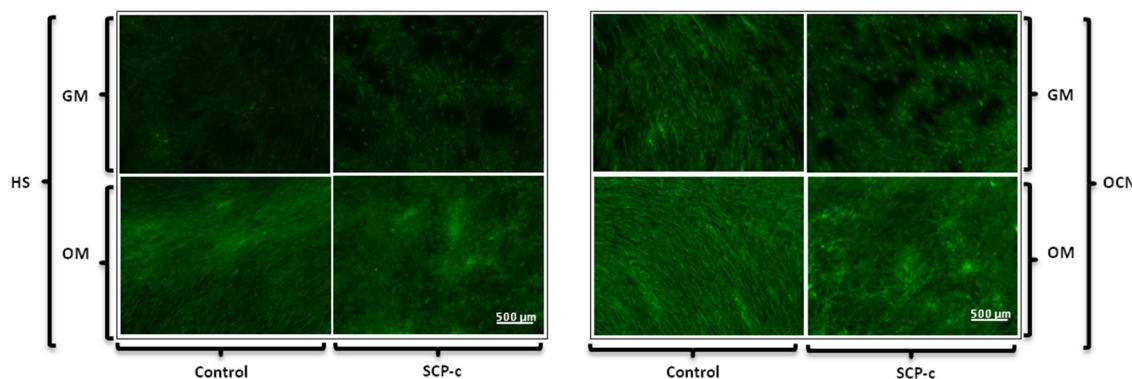


Figure 3. Representative immunofluorescence staining of Collagen I (Col I), Osteopontin (OPN), Heparan Sulphate (HS) and Osteocalcin (OCN) images (magnification: bar 500 μ m) of the *ah*MSCs seeded in plastic (control) and cells growing in indirect contact with a Porous Si-Ca-P Monophasic Ceramic (SCP-c) at 28 days with growth medium (GM) or osteogenic medium (OM).

4.3.2. Surface Markers CD

Flow cytometric analysis was used in order to examine the presence of CD90, CD73 and CD105 surface antigens on *ah*MSCs (Figure 4). A total of 8.56% of the *ah*MSCs seeded in indirect contact with SCP-c lost CD90 antigen after 28 days in culture with OM, whereas only 3.94% of the cells cultured in plastic lost this marker (Figure 4A,D). Similarly, there were differences in the loss of the cell marker CD 105 at 28 days after adding OM (Figure 4B,E). Over 16% of the cells grown in indirect contact with the material did not express CD105, being significantly higher ($p < 0.05$) than the loss of the cell marker CD105 in the cells seeded in plastic.

On the other hand, there were no differences in the expression of CD 73 (Figure 4C,F) between treatment (SCP-c) and control (plastic) during the studied experimental times.

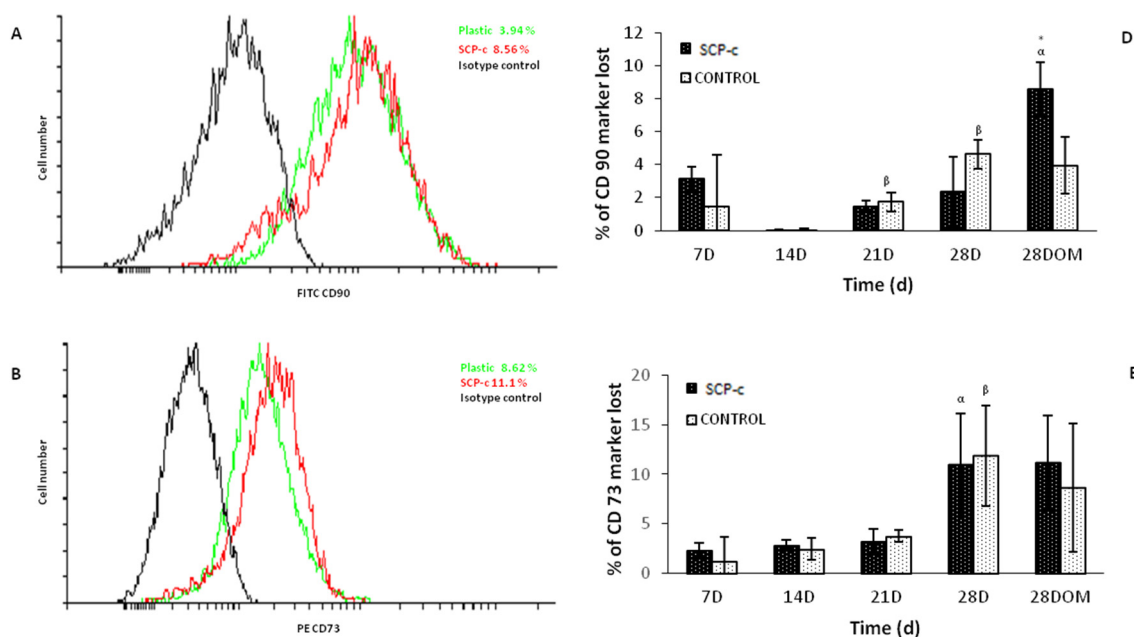


Figure 4. Cont.

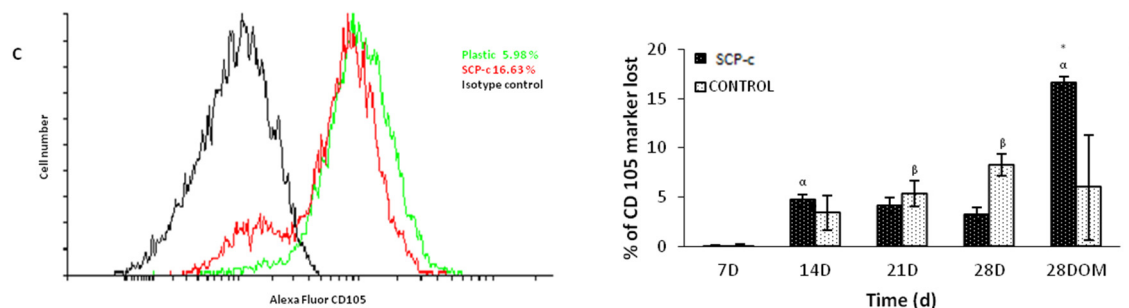


Figure 4. (A–C) Flow cytometry analysis of the expression of cell surface markers related to *ahMSCs* seeded on the SCP-c scaffolds compared to cell cultures on plastic and isotype control. (D–F) Percentage of surface marker lost with respect to the isotype control. (*) denotes significant differences ($p < 0.05$) between SCP-c and control at the same experimental time; (α) denotes significant differences ($p < 0.05$) between different experimental times obtained for cells growing on SCP-c scaffolds; (β) denotes significant differences ($p < 0.05$) between different experimental times obtained for control samples.

4.3.3. Quantitative Real-Time Polymerase Chain Reaction (qRT-PCR) Assay

The Pro-osteogenic effect on osteoblasts was further examined with respect to gene expression of IBSP, BGLAP, ALPL, SPP1, SPARC, RUNX2 and COL1A after 7, 14, 21 and 28 days in GM and 28 days of culture after replacing the GM by OM at 21 days. Figure 5 shows that genes associated with osteogenic differentiation including IBSP, ALPL, SPARC, SPP1 and COLI, were all significantly up-regulated in the SCP-c treatment ($p < 0.05$). In all groups, the osteogenic-related gene expression, except BGLAP and RUNX2, increased in a time-dependent manner.

The expression of gene RUNX2 seemed to increase at 28 days, but it was not significantly higher ($p > 0.05$). However, there were no differences between the expression of gene RUNX2 in control cells and *ahMSCs* in contact with SCP-c. In contrast to the other genes, BGLAP showed a continuous decrease from the 14th day in culture.

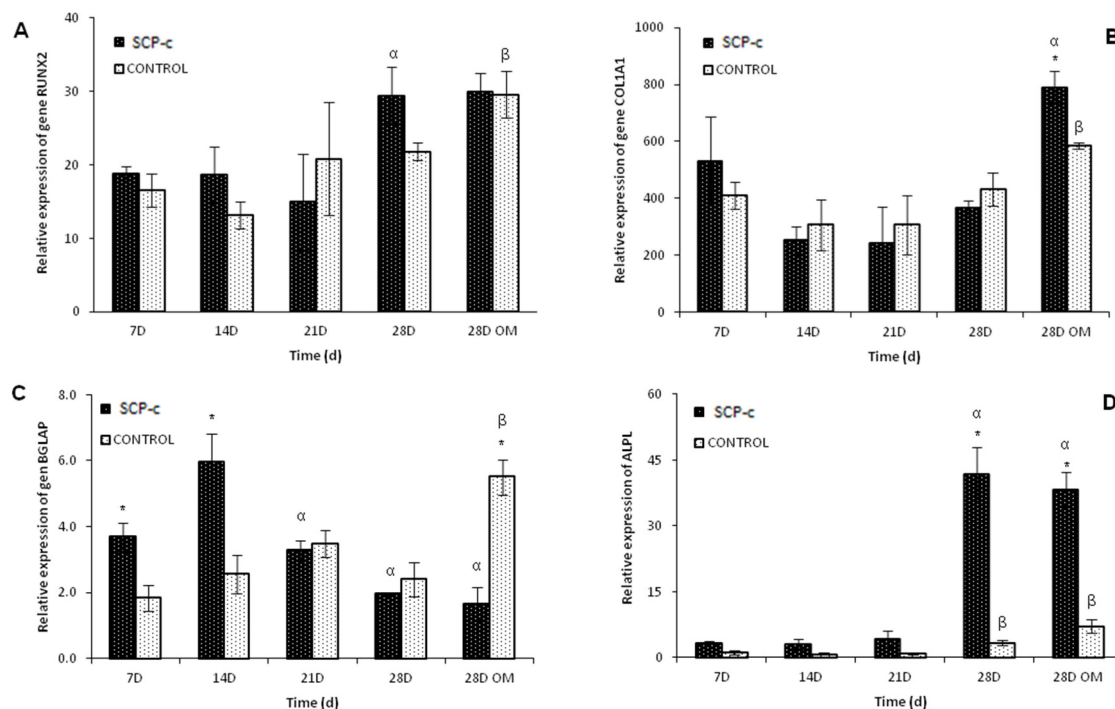


Figure 5. Cont.

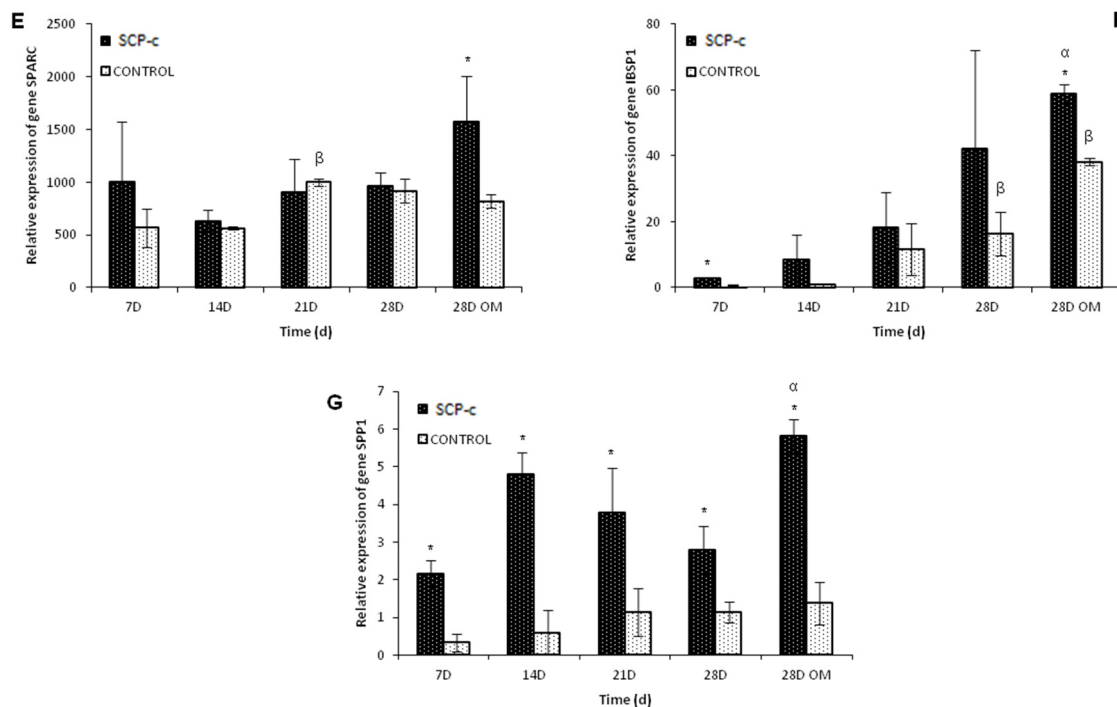


Figure 5. Real-time polymerase chain reaction (RT-PCR) was used to analyze the expression of genes RUNX2 (**A**), COL1A1 (**B**), BGLAP (**C**), ALPL (**D**), SPARC (**E**), IBSP1 (**F**) and SPP1 (**G**) in the cells seeded on the SCP-c scaffolds compared to cells cultured on plastic (positive controls). (*) denotes significant differences ($p < 0.05$) between SCP-c and the control for the same experimental time; (α) denotes significant differences ($p < 0.05$) between different experimental times obtained for cells growing on SCP-c scaffolds; (β) denotes significant differences ($p < 0.05$) between different experimental times obtained for control samples.

5. Discussion

Current treatment strategies for the repair or replacement of bone with synthetic implants and stem cells are a new approach to treat different conditions occurring in the medical field. The fabrication of ceramic scaffolds adding the use of autologous *ah*MSCs is aimed at transplantation to a large bone defect site observed in some clinical conditions such as tumour surgery, infections, implant rescue in orthopaedic and oral surgery [2]. An ideal biomaterial scaffold designed for bone tissue engineering must be degraded over time into non-toxic products and requires osteoconductive, osteoinductive and osteogenic properties.

Adding inorganic elements to scaffolds could significantly improve the bioactivity of materials as previously seen with bioglass, bioceramics that contain CaO, SiO₂ and P₂O₅ or glass-ceramic [19,20]. Also, these constructs could include additional growth factors or incorporate undifferentiated MSCs [21].

The osteoinduction of the materials was tested in this study, verifying their ability to lead *ah*MSCs toward an osteoblastic lineage differentiation.

Firstly, we examined the shape of the cells cultured on SCP-c by FESEM and their metabolic activity. Theoretically, cells will be spherical initially, then flatten and later sufficiently spread out so that the nucleus becomes prominent [17,22]. In our experiments, cells attached and adhered on SCP-c were found to be more spread out when they were cultured with OM. It has been noted that changes in expression of integrins, cadherins, and cytoskeletal proteins that occurs in the differentiation of stem cells produce cell morphological changes [23]. Moreover, previous studies have suggested that changes in cell shape can regulate the degree of development of lineage-specific markers, or differentiation, in precommitted preadipocytes or preosteoblasts [24,25]. For all this, it is possible the morphological

changes observed are related to the differentiation of cells. Remarkably, *ah*MSCs cultured on SCP-c with OM showed major metabolic activity than cells cultured with GM after 28 days. Upon osteogenic induction, the copy number of mitochondrial DNA, protein subunits of the respiratory enzymes, oxygen consumption rate and intracellular ATP content are increased, indicating the upregulation of aerobic mitochondrial metabolism [26]. Therefore, a greater metabolic activity could be related to cellular differentiation mechanisms.

The presence of the surface markers CD 105, 90, and 73 is considered as fundamental during the characterization and isolation of *ah*MSCs [27]; these markers were previously used by our research group to characterize *ah*MSCs from mononucleated fraction obtained by SEPAX isolation. The analysis of the cell surface markers showed that cells seeded in indirect contact with SCP-c exhibited a reduction of the expression of CD 105 and CD 90; this fact can be considered a consequence of the differentiation program activation [28].

A common method to evaluate the potential osteoinductivity of a novel biomaterial is to establish genetic expression profiles related to differentiation. In this case, the genes of interest are those implicated in osteogenic differentiation, from the first stages, such as APL or Col I [29], to those expressed in the late phase of this process and considered markers of osteoblastic cell differentiation [30], for example OCN.

Among these genes, the RUNX2 transcription factor is known to play a key role in osteoblastic differentiation [31] because it can directly stimulate transcription of OCN, Col I, OPN and collagenase III genes binding to the sequence PuCCPuCA. Beyond this, the molecular mechanism of RUNX2 action is still unknown. Although RUNX2 is expressed exclusively in mineralized tissues and their precursors, in many cases there may be no correlation between their expression and the expression of osteoblast-related genes. It has been demonstrated that inconsistencies between Runx2 mRNA or protein levels and its transcriptional activity suggests that posttranslational modification and/or protein-protein interactions may regulate this factor [32].

The results of the qRT-PCR experiments show that the RUNX2 gene is not upregulated in cells seeded on SCP-c materials or the control. The addition of the OM does not increase RUNX2 expression, but OPN or IBSP expression increases in samples incubated with the materials, indicating the participation of RUNX2 in guiding the expression of these markers. RUNX2 mRNA variations are not correlated with OPN or IBSP levels, probably because the RUNX2 protein is active after post-transcriptional or post-translational modifications [33,34].

ALP activity increased in cells incubated with SCP-c materials 28 days after the seeding with GM and OM, which is concordant with the maximum release of silicon to the medium previously stated by our group [14]. It has been widely proved that silicon plays an important role promoting cell proliferation [11], ALP expression and mineralization [35]. On the other hand, ALP activity can be influenced by calcium levels, which in small amounts cause the increase of ALP activity and cell differentiation. Moreover, osteogenic supplements, like ascorbic acid and β -glycerophosphate, up-regulate ALP gene expression [36]. Osteogenic supplements in OM, low concentrations of Ca and increasing levels of Si from 21 days to 28 days may create a synergistic effect on the stimulation of ALP activity.

The formation and maturation of the extracellular matrix (ECM) are also studied as markers of osteoblastic differentiation. Col I and SPARC are both markers of early osteoblastic differentiation [37]. Their mRNA expression seemed to be influenced by the Si-Ca-P monophasic ceramic in this study from first week to the last week by adding OM at 28 days. *ah*MSCs express high levels of Col I in their in vivo natural environment [38]. qRT-PCR results for Col I were confirmed by Col I immunofluorescence images. In fact, Col I seemed to be synthesized since the first stages of ECM deposition in all the samples considered, and it increased after adding OM at 28 days.

During the fourth week, SCP-c also was able to upregulate the markers of a more mature extracellular matrix, such as OPN and IBSP1, whose role is to influence and regulate mineralization processes. The qRT-PCR results showed that cells seeded under the influence of SCP-c reached the

maximum expression of these mRNA markers during the fourth week with the best performance in presence of the OM. These data are in accordance with the results stated by Kulterer B et al. [39] in the genetic expression profiles obtained for *ahMSCs* during osteoblastic differentiation studies. OPN qRT-PCR results are confirmed by the results of the immunofluorescence study. During the last week of culture, OPN proteins are highly expressed in the samples incubated with the material, demonstrating that the ECM is maturing, as expected.

HA and β -TCP are highly biocompatible, but differ in their biological response at the implantation site. While HA does not significantly degrade, and remains permanent over time, β -TCP has been shown to be a reabsorbable and osteoconductive material [40,41]. For decades, β -TCP has been widely used for repairing small bone defects, proving an environment where osteoblasts and MSCs are able to proliferate, providing an adequate matrix for bone formation [41–44]. Based on its gradually reabsorption and its proven osteoinduction properties, we think that the SCP-c material could be used as an alternative to natural bone.

6. Conclusions

Differentiation osteogenic markers were more intense in cells growing under the influence of SCP-c material, but specially after adding OM. All these results could indicate that the ceramic will be able to induce cell differentiation in the presence of other osteogenic supplements that we can find naturally in organisms.

Future studies will be focused on determining the *in vivo* properties of this bioceramic and improvements of its composition by adding different molecules such growth factors, drugs or coatings.

Acknowledgments: Part of this work was supported by the Spanish Ministry of Economy and Competitiveness (MINECO) contract grant number: MAT2013-48426-C2-2-R. Aznar-Cervantes Salvador acknowledges the financial support of his research contract, program INIA-CCAA (DOC INIA 2015), announced by the National Institute for Agricultural and Food Research and Technology (INIA) and supported by The Spanish State Research Agency (AEI) under the Spanish Ministry of Economy, Industry and Competitiveness

Author Contributions: Meseguer-Olmo Luis. and De Aza Piedad N. conceived and designed the experiments; Rabadan-Ros Ruben and Revilla-Nuin Beatriz performed the experiments; Mazón Patricia and Ros-Tarraga Patricia performed the preparation of the ceramics; Rabadan-Ros Ruben, Aznar-Cervantes Salvador, De Aza Piedad N. and Meseguer-Olmo Luis. wrote the paper. All authors contributed to the analyses and discussion of the results.

Conflicts of Interest: The authors declare no conflict of interest.

References

1. Boyan, B.D.; Hummert, T.W.; Dean, D.D.; Schwartz, Z. Role of material surfaces in regulating bone and cartilage cell response. *Biomaterials* **1996**, *17*, 137–146. [[CrossRef](#)]
2. Bosetti, M.; Cannas, M. The effect of bioactive glasses on bone marrow stromal cells differentiation. *Biomaterials* **2005**, *26*, 3873–3879. [[CrossRef](#)] [[PubMed](#)]
3. Lugo, G.; Mazón, P.; De Aza, P. Phase transitions in single phase Si–Ca–P-based ceramic under thermal treatment. *J. Eur. Ceram. Soc.* **2015**, *35*, 3693–3700. [[CrossRef](#)]
4. Puppi, D.; Chiellini, F.; Piras, A.; Chiellini, E. Polymeric materials for bone and cartilage repair. *Prog. Polym. Sci.* **2010**, *35*, 403–440. [[CrossRef](#)]
5. Hild, N.; Schneider, O.D.; Mohn, D.; Luechinger, N.A.; Koehler, F.M.; Hofmann, S.; Vetsch, J.R.; Thimm, B.W.; Müller, R.; Stark, W.J. Two-layer membranes of calcium phosphate/collagen/plga nanofibres: In vitro biominerallisation and osteogenic differentiation of human mesenchymal stem cells. *Nanoscale* **2011**, *3*, 401–409. [[CrossRef](#)] [[PubMed](#)]
6. Duan, Y.; Zhang, Z.; Wang, C.; Chen, J.; Zhang, X. Dynamic study of calcium phosphate formation on porous HA/TCP ceramics. *J. Mater. Sci. Mater. Med.* **2004**, *15*, 1205–1211. [[CrossRef](#)] [[PubMed](#)]
7. Pan, H.; Zhao, X.; Darvell, B.W.; Lu, W.W. Apatite-formation ability–predictor of “bioactivity”? *Acta Biomater.* **2010**, *6*, 4181–4188. [[CrossRef](#)] [[PubMed](#)]
8. Jonasova, L.; Müller, F.A.; Helebrant, A.; Strnad, J.; Greil, P. Hydroxyapatite formation on alkali-treated titanium with different content of Na⁺ in the surface layer. *Biomaterials* **2002**, *23*, 3095–3101. [[CrossRef](#)]

9. Hoppe, A.; Güldal, N.S.; Boccaccini, A.R. A review of the biological response to ionic dissolution products from bioactive glasses and glass-ceramics. *Biomaterials* **2011**, *32*, 2757–2774. [CrossRef] [PubMed]
10. Valerio, P.; Pereira, M.M.; Goes, A.M.; Leite, M.F. The effect of ionic products from bioactive glass dissolution on osteoblast proliferation and collagen production. *Biomaterials* **2004**, *25*, 2941–2948. [CrossRef] [PubMed]
11. Shie, M.-Y.; Ding, S.-J.; Chang, H.-C. The role of silicon in osteoblast-like cell proliferation and apoptosis. *Acta Biomater.* **2011**, *7*, 2604–2614. [CrossRef] [PubMed]
12. Rabadan-Ros, R.; Mazón, P.; Serena, S.; Sainz, M.; Meseguer-Olmo, L.; De Aza, P. In vitro behaviour of nurse's a ss-phase: A new calcium silicophosphate ceramic. *J. Eur. Ceram. Soc.* **2017**, *37*, 2943–2952. [CrossRef]
13. Rabadan-Ros, R.; Velásquez, P.A.; Meseguer-Olmo, L.; De Aza, P.N. Morphological and structural study of a novel porous nurse's a ceramic with osteoconductive properties for tissue engineering. *Materials* **2016**, *9*, 474. [CrossRef] [PubMed]
14. Rabadan-Ros, R.; Aznar-Cervantes, S.; Mazón, P.; Ros-Tarraga, P.; De Aza, P.N.; Meseguer-Olmo, L. Nurse's a-phase material enhance adhesion, growth and differentiation of human bone marrow-derived stromal mesenchymal stem cells. *Materials* **2017**, *10*, 347. [CrossRef] [PubMed]
15. Lugo, G.J.; Mazón, P.; Piedad, N. Material processing of a new calcium silicophosphate ceramic. *Ceram. Int.* **2016**, *42*, 673–680. [CrossRef]
16. Lugo, G.J.; Mazón, P.; Baudin, C.; De Aza, P.N. Nurse's a-phase: Synthesis and characterization in the binary system Ca_2SiO_4 – $\text{Ca}_3(\text{PO}_4)_2$. *J. Am. Ceram. Soc.* **2015**, *98*, 3042–3046. [CrossRef]
17. De Aza, P.N.; García-Bernal, D.; Cragnolini, F.; Velasquez, P.; Meseguer-Olmo, L. The effects of Ca_2SiO_4 – $\text{Ca}_3(\text{PO}_4)_2$ ceramics on adult human mesenchymal stem cell viability, adhesion, proliferation, differentiation and function. *Mater. Sci. Eng. C Mater. Biol. Appl.* **2013**, *33*, 4009–4020. [CrossRef] [PubMed]
18. Dominici, M.; Le Blanc, K.; Mueller, I.; Slaper-Cortenbach, I.; Marini, F.; Krause, D.; Deans, R.; Keating, A.; Prockop, D.; Horwitz, E. Minimal criteria for defining multipotent mesenchymal stromal cells. The international society for cellular therapy position statement. *Cytotherapy* **2006**, *8*, 315–317. [CrossRef] [PubMed]
19. García-Páez, I.H.; Carrodeguas, R.G.; Antonio, H.; Baudín, C.; Pena, P. Effect of Mg and Si co-substitution on microstructure and strength of tricalcium phosphate ceramics. *J. Mech. Behav. Biomed. Mater.* **2014**, *30*, 1–15. [CrossRef] [PubMed]
20. Taherkhani, S.; Moztarzadeh, F. Influence of strontium on the structure and biological properties of sol-gel-derived mesoporous bioactive glass (MBG) powder. *J. Sol-Gel Sci. Technol.* **2016**, *78*, 539–549. [CrossRef]
21. Giannoudis, P.V.; Dinopoulos, H.; Tsiridis, E. Bone substitutes: An update. *Injury* **2005**, *36*, S20–S27. [CrossRef] [PubMed]
22. Nair, M.B.; Varma, H.; John, A. Triphasic ceramic coated hydroxyapatite as a niche for goat stem cell-derived osteoblasts for bone regeneration and repair. *J. Mater. Sci. Mater. Med.* **2009**, *20*, 251–258. [CrossRef] [PubMed]
23. McBeath, R.; Pirone, D.M.; Nelson, C.M.; Bhadriraju, K.; Chen, C.S. Cell shape, cytoskeletal tension, and rhoa regulate stem cell lineage commitment. *Dev. Cell* **2004**, *6*, 483–495. [CrossRef]
24. Sordella, R.; Jiang, W.; Chen, G.-C.; Curto, M.; Settleman, J. Modulation of rho gtpase signaling regulates a switch between adipogenesis and myogenesis. *Cell* **2003**, *113*, 147–158. [CrossRef]
25. Thomas, C.H.; Collier, J.H.; Sfeir, C.S.; Healy, K.E. Engineering gene expression and protein synthesis by modulation of nuclear shape. *Proc. Natl. Acad. Sci. USA* **2002**, *99*, 1972–1977. [CrossRef] [PubMed]
26. Chen, C.T.; Shih, Y.R.V.; Kuo, T.K.; Lee, O.K.; Wei, Y.H. Coordinated changes of mitochondrial biogenesis and antioxidant enzymes during osteogenic differentiation of human mesenchymal stem cells. *Stem Cells* **2008**, *26*, 960–968. [CrossRef] [PubMed]
27. Conget, P.A.; Minguell, J.J. Phenotypical and functional properties of human bone marrow mesenchymal progenitor cells. *J. Cell. Physiol.* **1999**, *181*, 67–73. [CrossRef]
28. Mafi, P.; Hindocha, S.; Mafi, R.; Griffin, M.; Khan, W. Adult mesenchymal stem cells and cell surface characterization—A systematic review of the literature. *Open Orthop. J.* **2011**, *5*, 253–260. [CrossRef] [PubMed]
29. Setzer, B.; Bächle, M.; Metzger, M.C.; Kohal, R.J. The gene-expression and phenotypic response of hfob 1.19 osteoblasts to surface-modified titanium and zirconia. *Biomaterials* **2009**, *30*, 979–990. [CrossRef] [PubMed]

30. Harada, S.-I.; Rodan, G.A. Control of osteoblast function and regulation of bone mass. *Nature* **2003**, *423*, 349–355. [CrossRef] [PubMed]
31. Ducy, P.; Zhang, R.; Geoffroy, V.; Ridall, A.L.; Karsenty, G. Osf2/cbfa1: A transcriptional activator of osteoblast differentiation. *Cell* **1997**, *89*, 747–754. [CrossRef]
32. Lee, K.-S.; Kim, H.-J.; Li, Q.-L.; Chi, X.-Z.; Ueta, C.; Komori, T.; Wozney, J.M.; Kim, E.-G.; Choi, J.-Y.; Ryoo, H.-M. Runx2 is a common target of transforming growth factor β 1 and bone morphogenetic protein 2, and cooperation between RUNX2 and SMAD5 induces osteoblast-specific gene expression in the pluripotent mesenchymal precursor cell line c2c12. *Mol. Cell. Biol.* **2000**, *20*, 8783–8792. [CrossRef] [PubMed]
33. Franceschi, R.T.; Xiao, G. Regulation of the osteoblast-specific transcription factor, runx2: Responsiveness to multiple signal transduction pathways. *J. Cell. Biochem.* **2003**, *88*, 446–454. [CrossRef] [PubMed]
34. Franceschi, R. The developmental control of osteoblast-specific gene expression: Role of specific transcription factors and the extracellular matrix environment. *Crit. Rev. Oral Biol. Med.* **1999**, *10*, 40–57. [CrossRef] [PubMed]
35. Dong, M.; Jiao, G.; Liu, H.; Wu, W.; Li, S.; Wang, Q.; Xu, D.; Li, X.; Liu, H.; Chen, Y. Biological silicon stimulates collagen type 1 and osteocalcin synthesis in human osteoblast-like cells through the BMP-2/SMAD/RUNX2 signaling pathway. *Biol. Trace Elem. Res.* **2016**, *173*, 306–315. [CrossRef] [PubMed]
36. Cheng, S.-L.; Yang, J.W.; Rifas, L.; Zhang, S.-F.; Avioli, L.V. Differentiation of human bone marrow osteogenic stromal cells in vitro: Induction of the osteoblast phenotype by dexamethasone. *Endocrinology* **1994**, *134*, 277–286. [CrossRef] [PubMed]
37. Jikko, A.; Harris, S.E.; Chen, D.; Mendrick, D.L.; Damsky, C.H. Collagen integrin receptors regulate early osteoblast differentiation induced by BMP-2. *J. Bone Miner. Res.* **1999**, *14*, 1075–1083. [CrossRef] [PubMed]
38. Schipani, E.; Kronenberg, H.M. *Adult Mesenchymal Stem Cells*; Harvard Stem Cell Institute: Cambridge, MA, USA, 2009.
39. Kulterer, B.; Friedl, G.; Jandrositz, A.; Sanchez-Cabo, F.; Prokesch, A.; Paar, C.; Scheideler, M.; Windhager, R.; Preisegger, K.-H.; Trajanoski, Z. Gene expression profiling of human mesenchymal stem cells derived from bone marrow during expansion and osteoblast differentiation. *BMC Genom.* **2007**, *8*, 70. [CrossRef] [PubMed]
40. Allabouch, A.; Colat-Parros, J.; Salmon, R.; Naim, S.; Meunier, J. Biocompatibility of some materials used in dental implantology: Histological study. *Coll. Surf. B Biointerfaces* **1993**, *1*, 323–329. [CrossRef]
41. Aybar, B.; Bilir, A.; Akçakaya, H.; Ceyhan, T. Effects of tricalcium phosphate bone graft materials on primary cultures of osteoblast cells in vitro. *Clin. Oral Implant. Res.* **2004**, *15*, 119–125. [CrossRef]
42. Liu, G.; Zhao, L.; Cui, L.; Liu, W.; Cao, Y. Tissue-engineered bone formation using human bone marrow stromal cells and novel β -tricalcium phosphate. *Biomed. Mater.* **2007**, *2*, 78–86. [CrossRef] [PubMed]
43. Payer, M.; Lohberger, B.; Stadelmeyer, E.; Bartmann, C.; Windhager, R.; Jakse, N. Behaviour of multipotent maxillary bone derived cells on β -tricalcium phosphate and highly porous bovine bone mineral. *Clin. Oral Implant. Res.* **2010**, *21*, 699–708. [CrossRef] [PubMed]
44. Yefang, Z.; Hutmacher, D.; Varawan, S.-L.; Meng, L.T. Comparison of human alveolar osteoblasts cultured on polymer-ceramic composite scaffolds and tissue culture plates. *Int. J. Oral Maxillofac. Surg.* **2007**, *36*, 137–145. [CrossRef] [PubMed]



© 2018 by the authors. Licensee MDPI, Basel, Switzerland. This article is an open access article distributed under the terms and conditions of the Creative Commons Attribution (CC BY) license (<http://creativecommons.org/licenses/by/4.0/>).